

Comparison between AC and MF-DC resistance spot welding by using high speed filming

S.C.A. Alfaro^a

co-operating with

J.E. Vargas^{a,*}, **M.A. Wolff**^b, **L.O. Vilarinho**^b

^a Graco, University of Brasilia, Brasilia, Brazil

^b Laboratory for Welding Process Development – Laprosolda, Federal University of Uberlandia, Brazil

* Corresponding author: E-mail address: jevargas@hotmail.com

Received 30.03.2007; published in revised form 01.09.2007

Manufacturing and processing

ABSTRACT

Purpose: In this work it will be carried through the filming of the formation and growth of the nugget in resistance spot welding executed in AC and MF. A comparison for same times in both the processes will be carried through to verify which of the used processes offers better conditions, control and results as well as will help for one better understanding of the process aiming at the otimização.

Design/methodology/approach: Two different spot welding machine (AC and MF-DC) had been used, and a digital high-speed camera. The weld points had been carried through in 3 galvanized steel different plate configurations. The electrodes had been truncated to obtain one better visualization for the weld nugget formation. The comparison of the formation and development between the weld point of each process (AC and MF) is shown in 7 pictures in the same values of time.

Findings: For currents below 2 kA, no nugget was observed. and the formation of same after 10° cycle for bigger current of 3 kA. The MF-DC welding offers the possibility of obtaining nuggets more uniforms within shorter times (depending on the plate configuration).

Research limitations/implications: In this work the AC machine is limited by the values of current of welding and pressure of the electrodes: (2 - 6) kA e (87 - 261) kgf respectively. Other materials: aluminum, stainless steel or material exactly dissimilar could be used following the line of this research. Bigger currents levels can also be used.

Originality/value: The idea to compare resulted for the same process of welding under different conditions (equipment, materials and or parameters) makes possible the choice of these better conditions used to the otimização of the process.

Keywords: Welding; Resistance spot welding; Nugget formation; High-speed filming

1. Introduction

The Resistance Spot Welding (RSW) is one of the most employed manufacturing processes in the automotive industry. In

this process, metal sheets are joined by the accomplishment of welded spots from the localized melting due to heat generated by the material resistance of current passage. The use of galvanized steels (hot-dip-galvanized, electrogalvanized and hot-dip-galvannealed), as a response against corrosion resistance and cost

reduction in tailored-blanks, brought difficulties while welding this material. Thus, the process quality has demanded new research lines, such as the fundamentals of the welding formation.

The scientific literature [1-4] has focused on the analysis, monitoring and improvement of the mechanisms for the weld nugget formation under different conditions, parameters and materials with the objective of welding process optimization. Dickinson et al. [1] and Kayser, et al. [2], among others, tried to understand the effects of the welding parameters on the formation and growth of the nugget in an attempt of better controlling these parameters for process optimization. Recently, Cho & Rhee [3] carried out a study by using a high-speed camera for monitoring the nugget growth and its relationship with the process parameters.

Accordingly to this presented research trend, it is aimed here to study the mechanism of the weld nugget formation by using high-speed visualization and, differently from other authors, keeping the same level of energy and synchronize with the electrical signals (current and voltage). Therefore, two different welding equipments are employed (alternate current – AC – power source and medium frequency constant current one – MF-DC) with three configurations of sheet thickness were employed (namely A, B and C).

The use of two power sources (AC and MF-DC) is justified due to the trend in industry for the replacement of AC by MF-DC equipment, in face of commercial claimed advantages from MF-DC over AC waves. Besides the inherent advantage of MF-DC adoption (smaller transformer, less secondary losses, etc), the manufacturers has underlined advantages, such as lower welding time, better parameter controlling and lower thermal-mechanical stress, despite of scientific studies.

2. Experimental procedure

The welding was made by two different spot welding machines. The alternate current one is composed by a transformer (manufacturer Soltronic HT75 2 MF, 440 V, 75 kVA, 170 A in the primary circuit) and a controller (manufacturer Fase Saldatura with maximum nominal power of 54 kVA) was used to supply a water-cooled electrodes with pneumatic pressure from 87 to 261 kgf, with the welding current (secondary circuit) varying from 2 to 8 kA and maximum welding cycle of 100.

The medium frequency direct current equipment has a PSG 3100 transformer, a PSI6100 (100L) controller and a pneumatic welding gun, also water-cooled. The welding current in the secondary varies from 1 up to 20 kA.

The welding pool visualization was carried out by using a digital high-speed camera (manufacturer Nac, model Memrecam CI V-145-J) set with F-mount lens (Nikon 90 mm, f#2.5 and 55 mm of diameter plus an UV lens). The illumination was made by a light source (model Arrilite 1000, with 1000 w, 60 Hz, 45°-250°C) in the spot mode (not in the flood mode). A rate of 1000 fps and a shutter time of 1/6000 s were set. The experimental rig is shown in Figure 1.

The electrodes (caps) are 16-mm external diameter, spherical type, Class A, Group 2, hardness of 75 HRb and 75% IACS. They

were truncated in a 3 mm of length and placed perpendicular to the sheet as shown in Figure 2a. This approach is necessary because if truncation is not made, the electrode tend to squeeze the spot. It also promotes a better visualization of the nugget formation (Figure 2b).

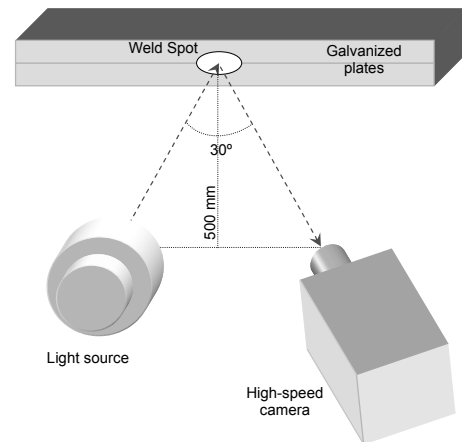


Fig. 1. Experimental rig

Since the final spot is not welded under a real situation, it must be built a relationship between a real situation and this approach for nugget visualization, which is represented in Figure 2b. This relationship must be performed under two criteria: same energy and same pressure levels. The same energy level is reached by applying Equation 1 that represents the heat generation by the Joule effect. Considering that the area in the visualization case is half of the one in a real spot welding ($A_2 = A_1/2$), by applying Equation 1 one finds that the current of the visualization case must be $I_2 = I_1/\sqrt{2}$. In the case of the electrode force (F_{el}), considering that the pressure upon the spots must remain the same and since the area becomes half of it, then the force should be half of the one in the first case ($F_2 = F_1/2$):

$$E = I_{rms}^2 \cdot R \cdot T_s = I_{rms}^2 \cdot \frac{\rho \cdot \ell}{A} \cdot T_s \quad (1)$$

where, E is the heat generated by the Joule effect in the sheets; I_{rms} is the true rms welding current; R is the sheet resistance; ρ is the sheet electrical resistivity; ℓ is the total sheet thickness; A is the spot area and T_s is the total welding cycle.

The metal sheets are hot-dip-galvanized and they are clamped together and the spot welding is carried out in the center of one side in order to guarantee repeatability. All sheets have dimension of 100 x 25 mm. Three different configurations are employed, namely A, B and C. Configuration A makes use of sheet thickness of 2.0 and 2.0 mm; configuration B uses sheets of 2.0 and 1.2 mm of thickness, whereas Configuration C employs sheet thickness of 1.2 and 1.2 mm. These sheets were sheared, deburred, aligned and isolated (from each other by a piece of paper in of the ends) in order to avoid shunt effects. The surfaces were cleaned up by detergent and dried in high-pressured air.

The welding procedure was carried out in two stages. The first one aimed to achieve a technological database for industrial application. Thus, operational envelopes were found. These envelopes characterize operational ranges varying from minimum values of current, force and cycles, where the joint is not accomplished, to maximum values where neither material expulsion nor deep depression (indentation) is observed. The second stage comes from the obtained operational envelopes, where five conditions were then selected for visualization of the nugget formation. The transposition from the welding conditions obtained from the operational envelopes (real situation) to the visualization case is made by applying the procedure described for Equation 1.

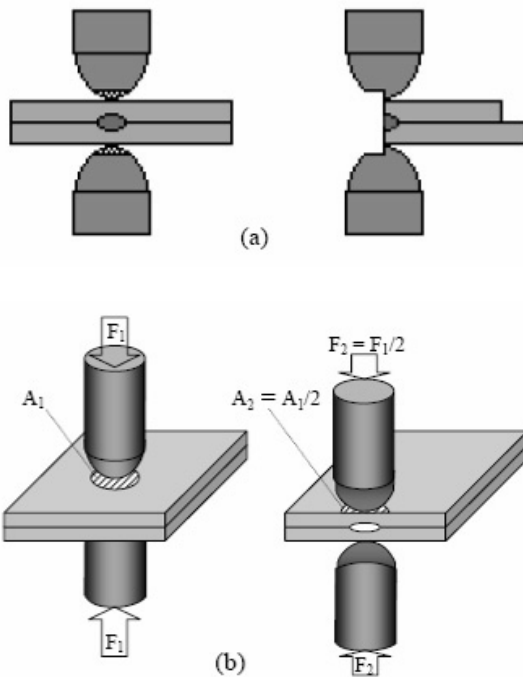


Fig. 2. (a) Sheets and caps location for welding procedure and (b) Geometrical aspects of comparing a real situation and the visualization one

3. Results and discussion

The obtained operational envelopes are shown in Figure 3. A total of six envelopes are presented for the three employed configuration of galvanized sheets; one brings rms current (I_{rms}) versus electrode force (F_e) curves and other rms current (I_{rms}) versus total welding cycle (T_s). In the first curves, a constant time of 30 cycles were employed, whereas the second curves, electrode force of 174 kgf were set. These two values were arbitrarily select and represent a situation where a good spot is obtained for the three sheets configurations. It must be pointed out that the electrical frequency is 60 Hz, i.e., the duration of one cycle is

equal to $1/60$ s or 16.7 ms, whereas for the MF-DC equipment, the welding cycles are defined directly in milliseconds.

From these six operational envelopes, five welding conditions were picked up to be characterized. They are shown in Tab. 1. Runs 4735, 4736 and 4737 represent the average central position of the envelopes, i.e., 5 kA; 174 kgf and 30 cycles (500 ms). As explained in Section 2, these values cannot be promptly used and must be respectively translated to 3.5 kA; 87 kgf and 30 cycles (500 ms). Runs 4739 and 4740 were made in order to trace a comparison with Run 4735 for investigating the effect of the rms current on the nugget formation.

Table 1.

Five selected conditions from the operation envelopes. The rms voltage (V_{rms}) was measured by the DAQ system. All runs are for 30 cycles and 87 kgf

Run	I_{rms} [A]	V_{rms} [V]	Plates Configuration
4735	3504	1,06	A
4736	3534	0,9	B
4737	3561	0,81	C
4739	2060	0,73	A
4740	3027	1,01	A

In the 4735 run (Figure 4), the first high-speed image presents the galvanized plates squeezed by the electrodes, without passing the welding current. The second image presents the first welding cycle, where the first melted drops start forming in the upper plate for both AC and MF-DC current. These droplets indicate the beginning of burning of the zinc coating. On the third image (10^{th} weld cycle) it can be observed a larger amount of melted zinc droplets, which starts being expelled from the nugget region. For the MF-DC current, it is possible to notice the nugget formation, which cannot be seeing for the AC process. On the fourth image (12^{th} weld cycle), the AC case presents a higher heating than previous image, while the MF-DC image presents a completed formed nugget. The nugget starts forming for the AC process in the fifth image (16^{th} weld cycle), i.e., delayed in respect to the MF-DC process. From the sixth image (21^{st} weld cycle), one can assert that the weld could have been stopped at this time, since the nugget is completed formed: it reached its maximum size and exaggerated plate deformation appears in the weld region. On this image is still possible to observe that after the accomplishment of half of the set weld cycles in the AC process, the nugget is still under formation. On the seventh image has the completion of the weld time (30^{th} weld cycle). From this image, it is possible to affirm that the weld time was excessively long for the MF-DC process, causing a large plate deformation in the welding region. However, this weld time was correctly set for the AC process.

In the 4736 run (Figure 5), the first and second images are similar to the ones in 4735 run. On the third image (10^{th} weld cycle), the nugget formation can be observed in the thicker plate, for both processes (AC and MF-DC), due to its higher electrical resistance. The nugget growth can be observed on the fourth image (12^{th} weld cycle). Oppositely to the previous run (4735), in this 4736 run the nugget growth is bigger for the AC process than in the MF one. Furthermore, in the MF-DC process, the thinner plate was not even melted. On the fifth image (16^{th} weld cycle), the nugget keep increasing for both processes. Also, the expulsion of zinc droplets from the coating is observed. The weld nugget.

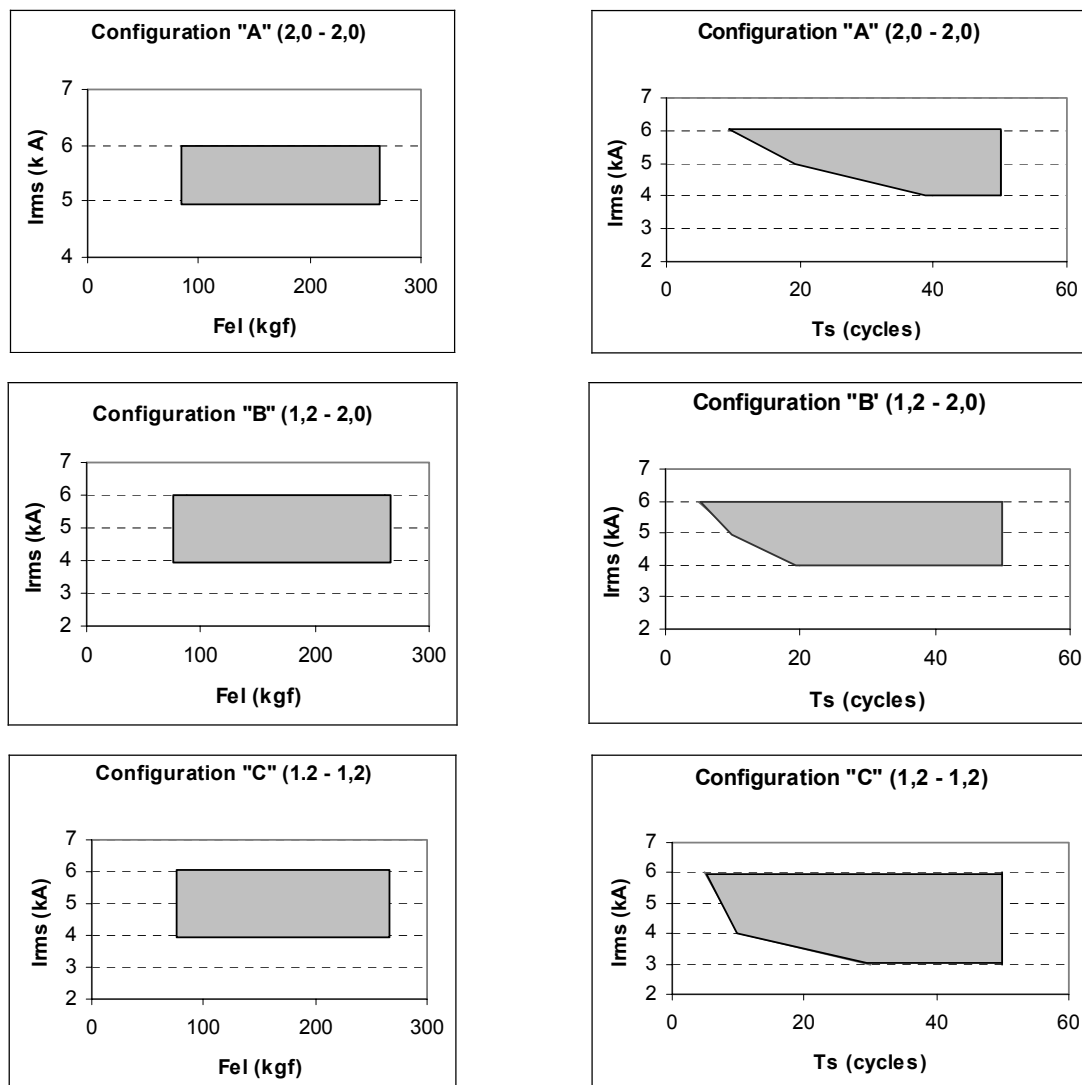


Fig. 3. Operational envelopes for both current x force (left) and current x total welding cycle (right)

reaches its maximum size in the 21st weld cycle (sixth image), and in the AC process, the melted material projection is imminent. The weld is done in the 30th weld cycle (seventh image), where the MF-DC process presents a well-defined and controlled nugget, without expulsion.

First and second images on Figure 6 are related to 4737 run and once again are similar to the ones already commented for 4735 run. On the third image (10th weld cycle) the nugget formation begins for both processes and for AC process the expulsion of melted material (projection) is verified. In the 12th weld cycle (fourth image), instability (spatter, projection and fumes) on the nugget formation is observed for AC process, whereas the nugget in MF-DC presents a smoothly growth.

Shifting in the nugget can be observed on the fifth image (16th weld cycle). This shift is clearly observed in the 21st cycle (sixth image) for the AC welding, where the nugget comes from the plates interface towards the electrode-plate interface. By this sixth

image is possible to assert that the nugget reaches its maximum size for the MF-DC process. The welding ends in the 30th cycle (seventh image), where superior quality is perceived for the nugget obtained by using MF-DC equipment rather than AC one.

The high speed images for 4739 run are presented on Figure 7. After the first and second images (already described for 4735 run), images number 3, 4, 5 and 6 show only the formation and expulsion of melted zinc droplets from the coating. However, the nugget formation is not present. On the seventh image (30th weld cycle) the process ends, but no weld nugget is formed; only color changing in the plates can be observed due to the heat input.

The last run (4740) has its high-speed images presented on Figure 8, where the first and second images were already described while discussing the 4735 run. In the 10th weld cycle (third image), the formation of melted zinc droplets is observed. These droplets are bigger for the AC process than the ones for the MF - DC welding. Also, pronounced color

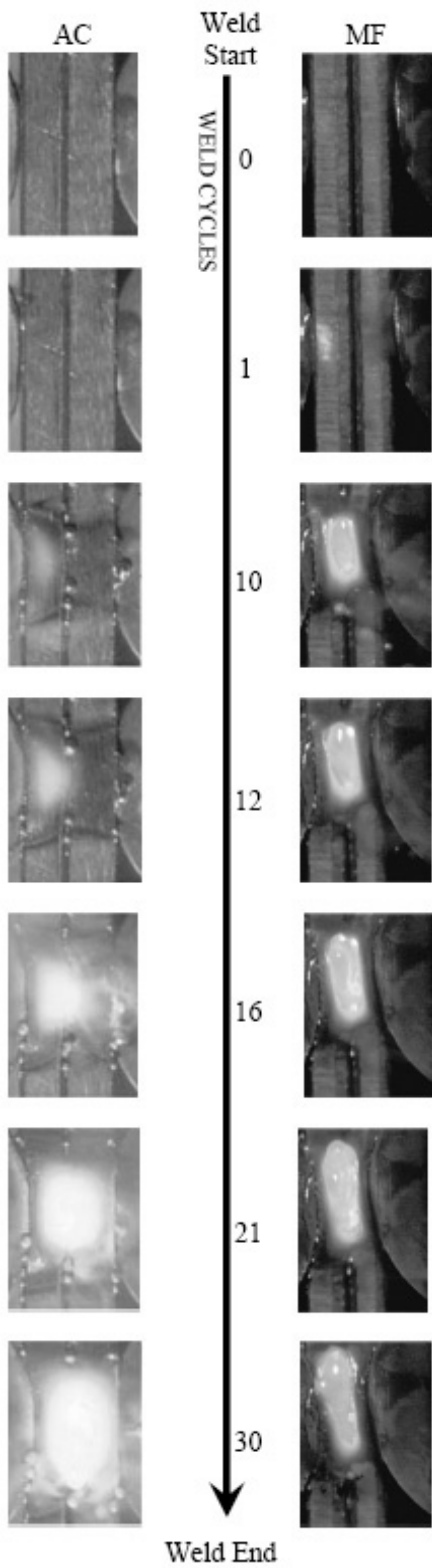


Fig. 4. High speed image sequence for 4735 run

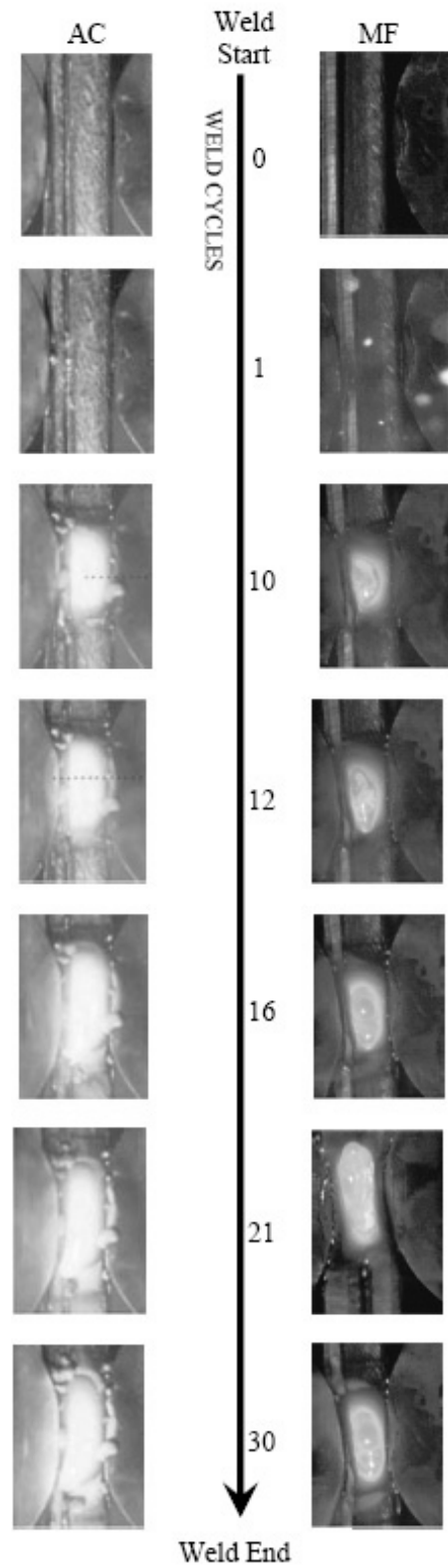


Fig. 5. High speed image sequence for 4736 run

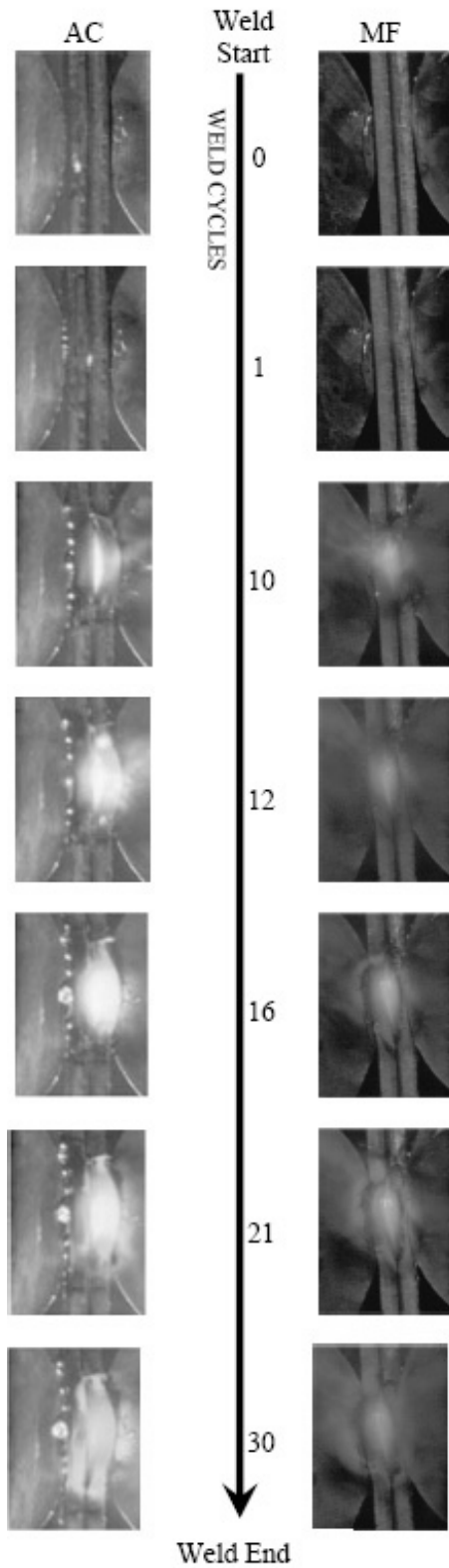


Fig. 6. High speed image sequence for 4737 run

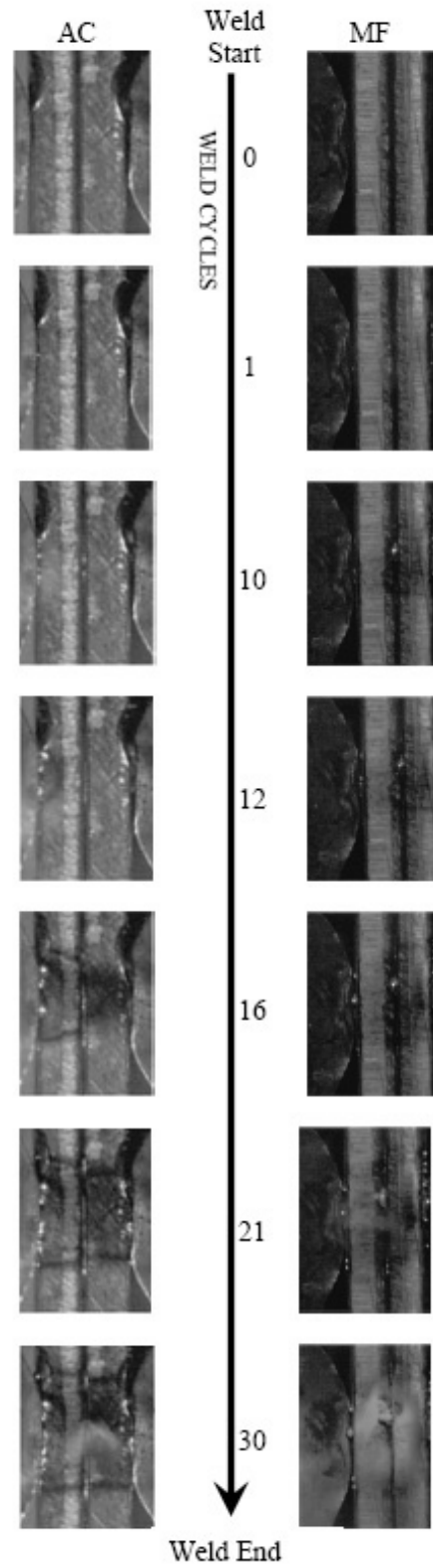


Fig. 7. High speed image sequence for and 4739 run

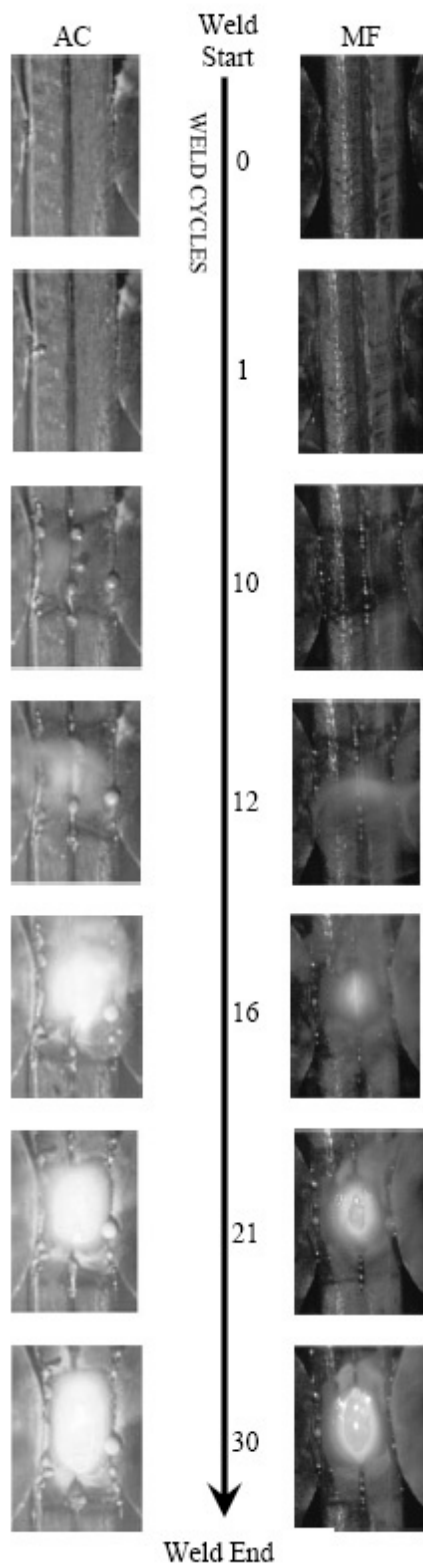


Fig. 8. High speed image sequence for 4740 run

changing is noticed for both processes. On the fourth image (12th weld cycle), the nugget is bigger for the AC process than for MF-DC one. In the 16th weld cycle (fifth image), a bulky nugget growth is observed with material expulsion for the AC process, whereas for the MF-DC welding the process is much more under control (nugget being formed in the plates interface). This characteristic of a controlled nugget formation for the MF-DC process is confirmed on the sixth image (21st weld cycle). On this image a bigger nugget is observed for the AC process. At the end of the welding (seventh image – 30th weld cycle), a smaller and higher quality nugget is observed for the MF-DC welding rather than AC process.

4. Conclusions

Practical and technological operational envelopes were presented for three different configurations of galvanized sheets jointed by RSW process with both AC and MF-DC equipment. Five runs were selected from these envelopes and then the nugget formation was visualized by high-speed images. From this procedure and the presented results it is possible to conclude that:

- The nugget size varies accordingly to the current oscillation (in this case 60 Hz);
- The higher the rms current the longer the solidification time of the nugget is required;
- The zinc coating starts to burn out by the first cycle for rms currents above 3 kA;
- Around the 16th cycle the coating no longer exists for rms currents above 3 kA;
- At the 10th welding cycle the nugget formation starts to be observed by a reddish area for rms currents above 3 kA;
- For rms currents below 2 kA, no nugget was observed.
- The MF-DC welding offers the possibility of obtaining nuggets more uniform within shorter times (depending on the plate configuration);
- The projection is reduced in the weld nugget (and therefore possible discontinuities) for the MF-DC welding.

References

- [1] D.W. Dickinson, J.E. Franklin A. Stanya, Characterization of spot welding behavior by dynamic electrical resistance monitoring, *Welding Journal* 59 (1980) 170-176.
- [2] J.G. Kayser, G.J. Dunn, T.W. Eagar, 1982, The effect of electrical resistance on nugget formation during spot welding, *Welding Journal* 61 (1982) 167-174.
- [3] Y. Cho, S. Rhee, 2003, Experimental Study of Nugget Formation in Resistance Spot Welding, *Welding Journal* 8 (2003) 195-201.
- [4] H.S. Cho, Y.J. Cho, A study of the thermal behavior in resistance spot welding, *Welding Journal* 68 (1989) 236-244.